Neuron, Volume *90*

Supplemental Information

Cannabinoid Type 2 Receptors Mediate a Cell Type-Specific Plasticity in the Hippocampus

A. Vanessa Stempel, Alexander Stumpf, Hai-Ying Zhang, Tuğba Özdoğan, Ulrike Pannasch, Anne-Kathrin Theis, David-Marian Otte, Alexandra Wojtalla, Ildikó Rácz, Alexey Ponomarenko, Zheng-Xiong Xi, Andreas Zimmer, and Dietmar Schmitz

Supplemental Materials

Supplemental Figures

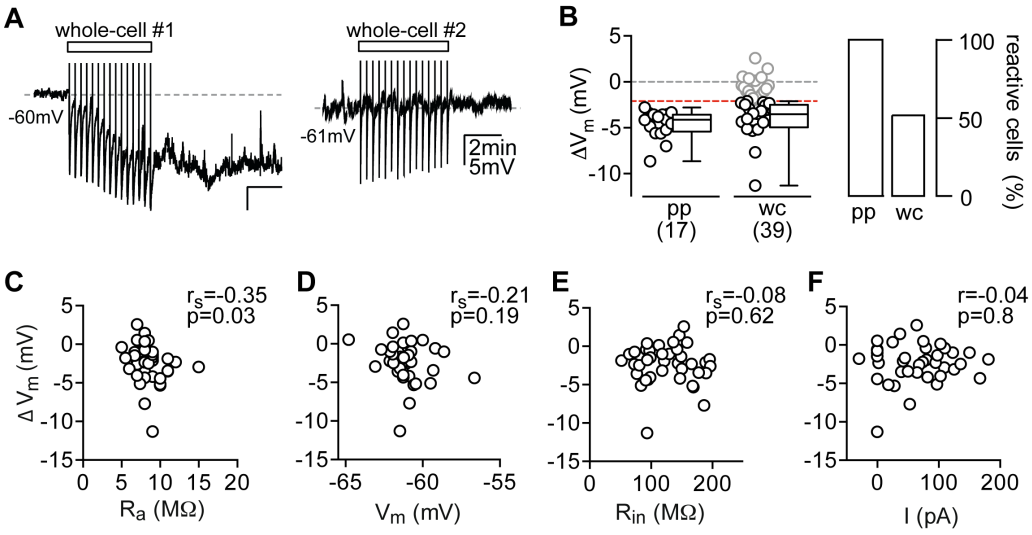

Figure S1. Related to Figure 1. Whole-cell recordings interfere with the V_m hyperpolarisation. (**A**) Whole-cell current-clamp recording of a reactive (left) and an unreactive CA3 PC (right) in response to the AP train stimulus (rectangle). (**B**) Left: the ΔV_m of each recorded cell (open circles) and the median, 25th and 75th percentile of the average ΔV_m recorded in the different recording conditions are shown for pp (data as in Fig. 1) and for n(N)=39(16) wc recordings (wc, with n=20 reactive cells: -3.5, -4.9 and -2.5mV). The dashed red line indicates the cut-off of -2.1mV by which cells were classified as reactive (black circles) or unreactive (grey circles). Right: % of reactive cells is shown for pp (100%) and wc (51.2%) recordings. (**C-F**) Correlation analysis of the ΔV_m and recording variables: The ΔV_m was significantly correlated to the R_a (C) but not the R_{in} (D), V_m (E) and the constant current injection needed to keep the cell at a holding potential of -60mV (F). Both the correlation coefficient (r or r_s) and the correlation's significance (p) are given for each correlation.

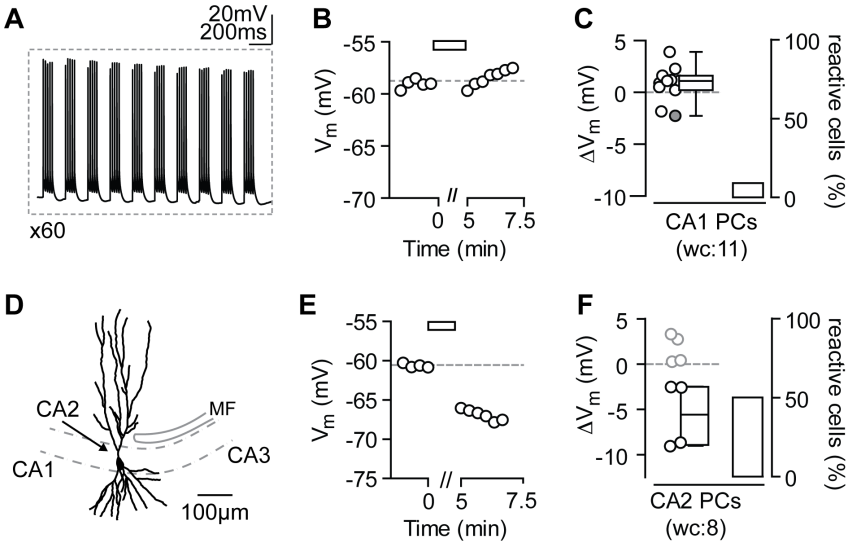

Figure S2. Related to Figure 1. Further analysis of cell-type specificity. (**A-C**) A theta-frequency burst protocol was used to elicit a total of 3000 action potentials in CA1 PCs recorded in wc configuration**.** (**A**) The first ten bursts in a recorded CA1 PCs are shown that were repeated 60x over 5 min. (**B**) The complete induction protocol (rectangle) did not induce a long-lasting hyperpolarisation in the same CA1 PC as can be seen in the time plot of its V_m. The V_m during the induction protocol is not included for display purposes. (**C**) Summary plot of n(N)=11(2) CA1 PCs with a ΔV_m (median, 25th and 75th percentile) of 1.12, 0.22 and 1.63mV (Wilcoxon test: P=0.64 compared to baseline). (**D-F**) CA2 PCs display a hyperpolarisation that is similar to CA3 PCs. (**D**) Anatomical reconstruction of a CA2 PC filled with 30µM Alexa. Note the characteristic bifurcation of the proximal dendritic tree (indicated by black arrow). The pyramidal cell layer is indicated by the dashed lines and the axonal projections from DG GCs, the mossy fibres (MF) that end at the border of CA3 to CA2, are shown in grey. (**E**) Time plot of the V_m of the same CA2 PC as in (D) in response to the action potential protocol (rectangle) recorded in wc configuration. The dashed line indicates the average baseline V_m. (**F**) The ΔV_m of each recorded cell (circles) and the median, 25th and 75th percentile of the average ΔV_m of all reactive cells are shown for (n(N)=8(5)) CA2 PCs: -5.8, -8.9 and -2.5mV (left). The percentage of reactive CA2 PCs was 50% (right).

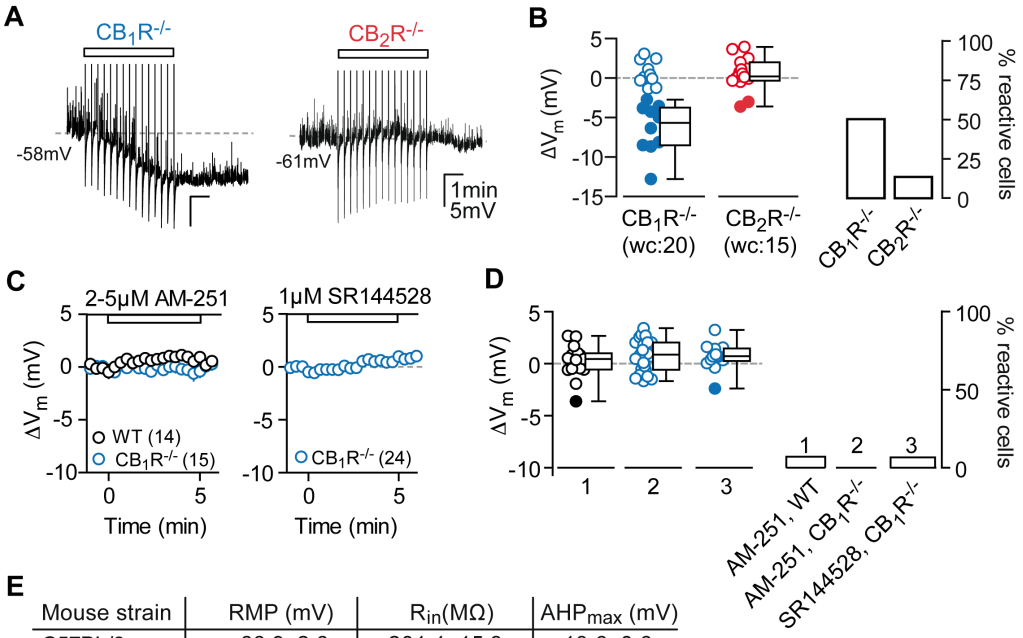

E

Mouse strain	RMP (mV)	R_{in}(MΩ)	AHP_{max} (mV)
C57BL/6	-66.9±2.6	201.1±15.8	-13.6±0.6
DAGLα KO	-65.5±1.9	260.1±26.9	-12.4±0.6
CB_1 R KO	-68.6±1.9	233.3±25.9	-13.3±1.3
CB_2R KO	-70.9±3	226.6±28.4	-12.8±1.9
Syn-CB_2 KO	-67.5±1.7	210.6±38.1	-10.8±1.1
	ns	ns	ns

Figure S3. Related to Figure 3. Cannabinoid receptor antagonists abolish the hyperpolarisation. (**A**) Whole-cell current-clamp recordings from both CB_1R and CB_2R KO animal lines confirm the results obtained in pp configuration as shown by the exemplary V_m traces of a $CB_1R^{-/-}$ (left) and $CB_2R^{-/-}$ CA3 PCs (right) recorded in wc configuration. (**B**) Left: summary box plot of the median ΔV_m (with 25th and 75th percentile) for reactive $CB_1R^{-/-}$ CA3 PCs (n(N)=20(5): -5.6, -8.5 and -3.7mV) and all $CB_2R^{-/-}$ CA3 PCs (n(N)=15(3): 0.21, -0.31 and 2mV). The V_m of $CB_2R^{-/-}$ CA3 PCs after the induction protocol did not differ significantly from baseline, whereas it did differ significantly for $CB_1R^{-/-}$ (paired t-test: P=0.45 and P=0.007 respectively). Right: the percentage of reactive cells for all recorded $CB_1R^{-/-}$ and $CB_2R^{-/-}$ CA3 PCs (50% vs. 13.3%). (**C**) Summary time course of the average ΔV_m in response to the action potential stimulus of whole-cell CA3 PCs recordings in slices of WT (n(N)=14(3)) and CB_1R KO mice (n(N)=15(3)) preincubated in the CBR antagonist 2-5μM AM-251 (left) and slices of CB_1R KO mice preincubated in the CB_2R-specific antagonist 1μM SR (right, n(N)=24(3)). (**D**) Left: the ΔV_m of each recorded cell (circles) and the median, 25thand 75th percentile of the average ΔV_m are shown for WT in AM-251 (0.72, 0.27 and 1.5mV), CB_1R KO in AM-251 (0.45, -0.56 and 1mV) and CB_1R KO in SR (0.88, -0.58 and 2.05mV). Right: the percentage of reactive CA3 PCs is shown for WT in AM-251 (7.1%), $CB_1R^{-/-}$ in AM-251 (0%) and $CB_1R^{-/-}$ in SR (6.7%). Filled circles indicate reactive cells. (**E**) Comparison of intrinsic electrophysiological parameters of CA3 PCs recorded in pp configuration revealed no significant differences between C57BL/6 WT and the different KO mouse strains.

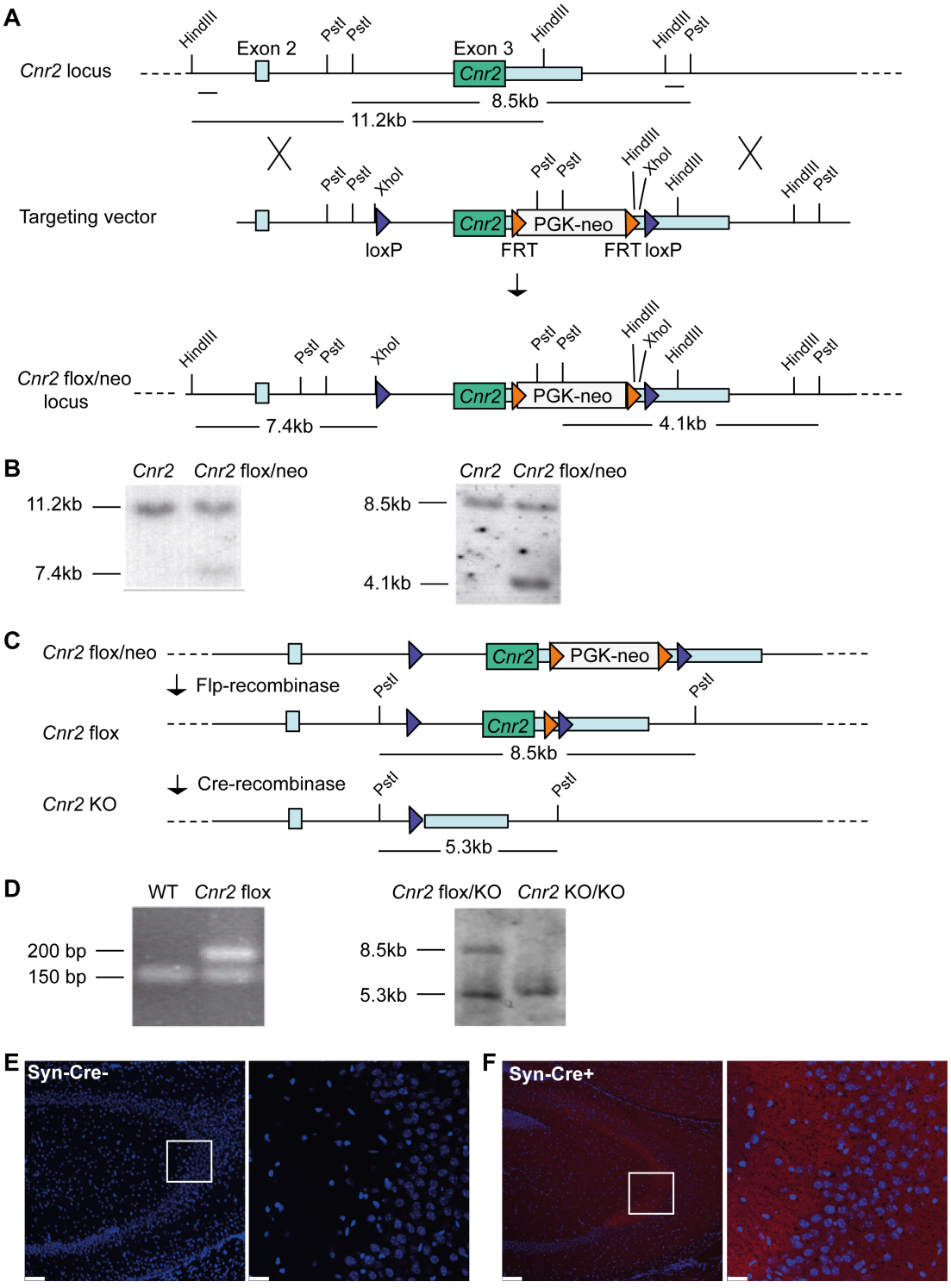

Figure S4. Related to Figure 3. Conditional Cnr2 targeting strategy. (**A**) *Cnr2* exons 2 and 3 are indicated as boxes, with the *Cnr2* coding region in dark green. The targeting vector contained a PGK-neo selection cassette, flanked by two FRT sites, in the 3' UTR. LoxP sequences were inserted in the intron between exons 2 and 3, as well as downstream of the PGK-neo cassette. (**B**) Recombinant ES cell clones were identified by Southern blotting with flanking 3' and 5' probes. (**C**) Mice carrying the *Cnr2* flox/neo locus were first crossed with a Flp-deleter mouse

strain, resulting in offspring with a *Cnr2* flox locus. (**D**) These animals are routinely genotyped by a PCR strategy. (**E-F**) Confocal images of the hippocampus of Syn-Cre- (E) and Rosa26-Stop-tdTomato-Syn-Cre+ reporter mice (F). Left panels: Overview of the hippocampus (scale bar: 100µm), right panels: higher magnification (scale bar: 25 µm) of area CA3. The confocal images clearly show the Syn-Cre expression in the hippocampus.

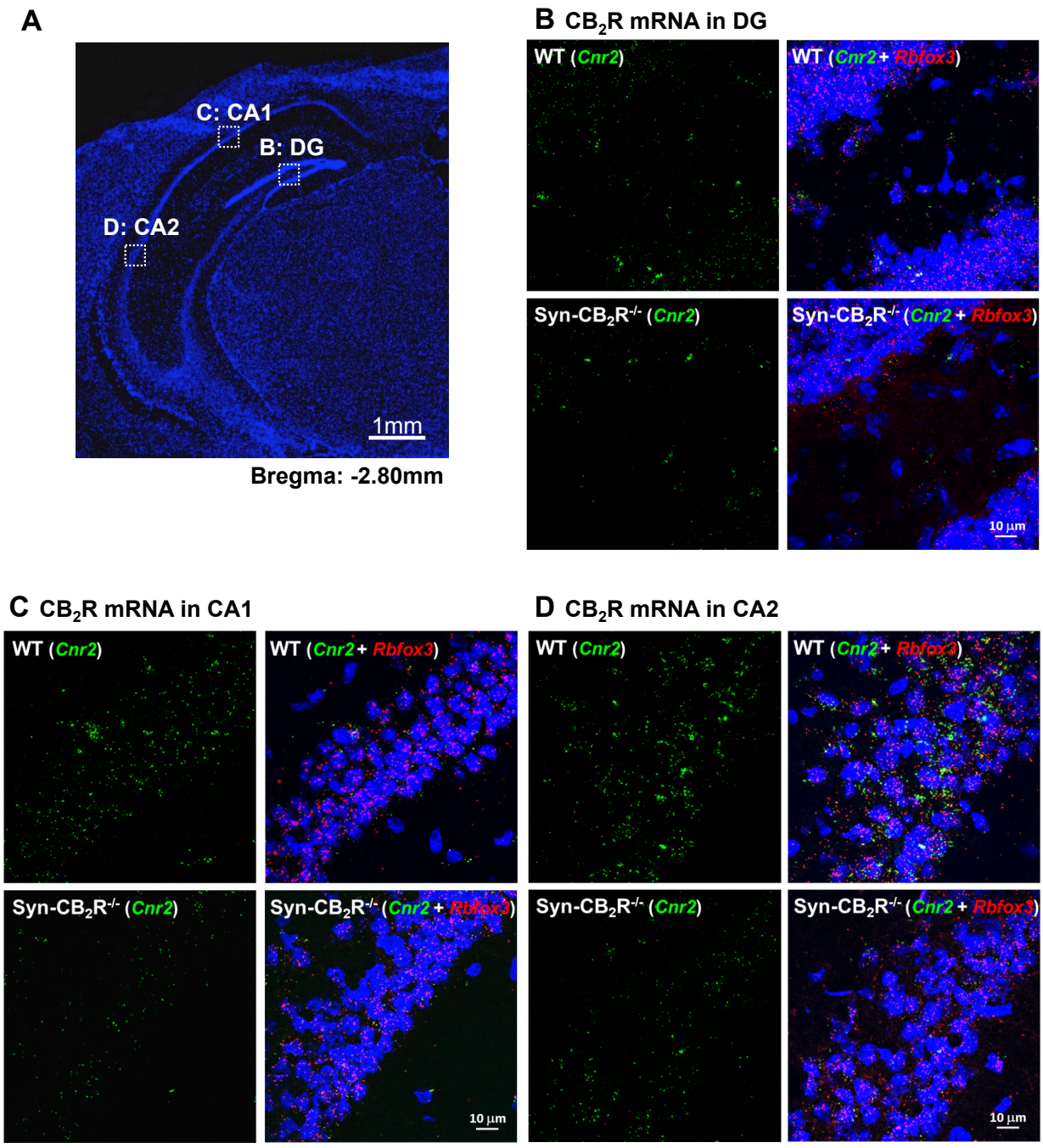

Figure S5. Related to Figure 4. CB_2R mRNA expression in the DG, CA1 and CA2 regions of the hippocampus as detected by RNAscope ISH. (**A**) Hippocampal image (DAPI staining), illustrating the target regions. (**B-D**) CB_2R mRNA (*Cnr2*, green) staining and co-localisation of CB_2R and NeuN (*Rbfox3*, red) mRNA in the DG (B), CA1 (C) and CA2 (D) of the hippocampus in WT (upper panels) and Syn-$CB_2R^{-/-}$ (lower panels) mice, illustrating a substantial reduction in CB_2R mRNA expression in Syn-CB_2R KO compared to WT mice. Note that the overall density of CB_2R mRNA in the DG and area CA1 is much lower than that in area CA2 or CA3 (see Figure 4).

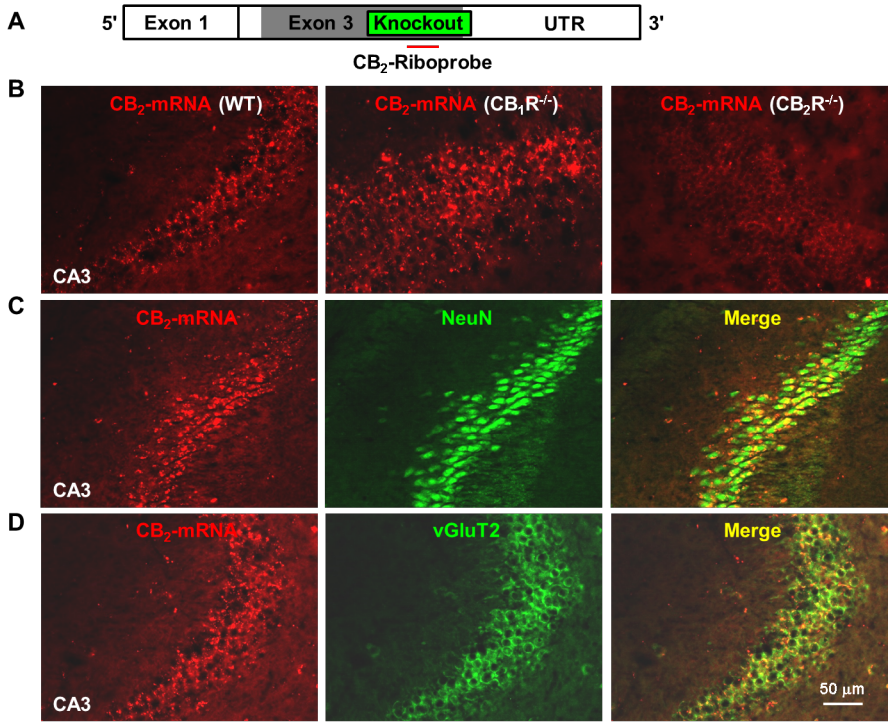

Figure S6. Related to Figure 4. CB_2R mRNA expression in area CA3 of mouse hippocampus by classical *ISH* assay. (**A**) The CB_2R mRNA structure in const. $CB_2R^{-/-}$ mice and the target region of a CB_2R probe used to detect CB_2R mRNA in the hippocampus of WT, $CB_1R^{-/-}$ and $CB_2R^{-/-}$ mice. This CB_2R-riboprobe targets the deleted region of the *Cnr2* gene in $CB_2R^{-/-}$ mice. (**B**) The CB_2R-riboprobe detected CB_2R mRNA in the CA3 region of hippocampus in WT and $CB_1R^{-/-}$, but not in $CB_2R^{-/-}$ mice. (**C-D**) Double-label fluorescent images, illustrating CB_2R mRNA (by ISH, red) is co-localised with NeuN (immunostaining, green) in hippocampal neurons (C) and also with vGluT2 (immunostaining, green) in hippocampal glutamatergic neurons (D) in WT mice.

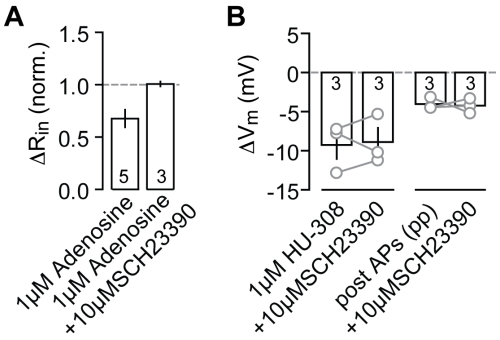

Figure S7. Related to Figure 5. Control of conductance-based R_{in} change mediated by adenosine-dependent activation of GIRK. (**A**) As a control, the relative change in R_{in} in response to 1µM Adenosine (n(N)=5(2): 0.67±0.08) is shown that was reversed by the application of the GIRK blocker 10µM SCH-23390 (1.01±0.02). (**B**) Acute application of SCH-23390 does not reverse the agonist- or AP-induced hyperpolarisation and thus excludes the involvement of GIRK channels. Left: single experiments (grey circles) and mean±SEM of n(N)=3(2) wc recordings showing the ΔV_m in HU and after SCH-23390 application (-9.3±1.8 and -8.9±1.8mV, paired t-test: P=0.82). Right: single experiments (grey circles) and mean±SEM of n(N)=3(2) pp recordings showing the ΔV_m after AP induction and with subsequent SCH-23390 application (-4±0.4 and -4.2±0.5mV, paired t-test: P=0.83).

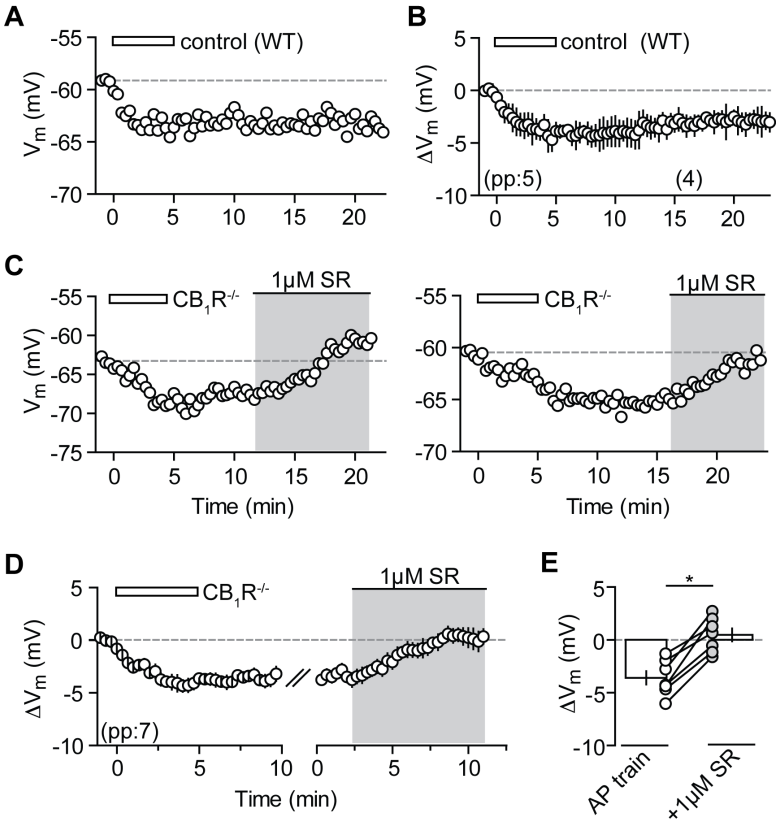

Figure S8. Related to Figure 6. Washin of the CB_2R inverse agonist SR acutely reverses the AP-induced hyperpolarisation. PP recordings of CA3 PCs in CB_1R KO and WT mice show that the V_m hyperpolarisation can be reversed by washin of 1µM SR. (**A**) Exemplary time plot of the V_m of a WT CA3 PC that was recorded for >15min post induction (AP train: rectangle). (**B**) Summary time plot of the average ΔV_m from n(N)=5(5) control WT CA3 PCs. At min15-20 the ΔV_m is still significantly different from baseline (-3.07±0.29mV; paired t-test: $p<0.05$). Note that this data is also included in Fig. 1. (**C**) Exemplary recordings of CB_1R-lacking CA3 PCs in which SR (grey) was washed in at different time points after the induction. (**D**) Summary time plot of n(N)=7(6) experiments in CB_1R KOs. (**E**) Before-after plot of each experiment showing the maximal ΔV_m after the AP train and the average ΔV_m of 10-15min after wash-in of SR. The mean average ΔV_m after the AP train (-3.6±0.63mV) after the AP train is significantly different from the mean ΔV_m after SR application (0.48±0.62mV; Wilcoxon matched pairs test: P=0.016). Furthermore, the V_m in SR does not differ from baseline values (Wilcoxon test: P=0.47).

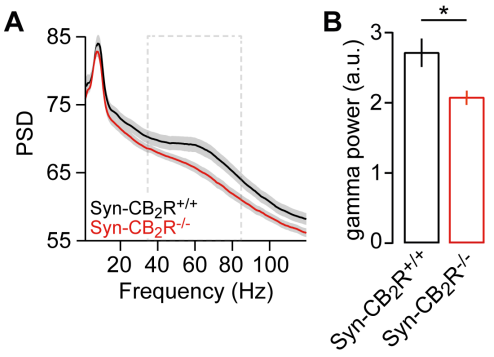

Figure S9. Related to Figure 8. Reduced power of gamma oscillations in area CA3 in Syn-$CB_2R^{-/-}$ mice. Average LFP power spectra (**A**) and cumulative power (**B**) in the 30-85Hz frequency band (grey rectangle in (A)) of control Syn-$CB_2R^{+/+}$ (n(N)=13(4)) and Syn-$CB_2R^{-/-}$ mice (n(N)=16(5), $F_{1,20}$=6.8, P=0.02). Data are presented as mean± SEM.

Supplemental Methods

Ethics statement and animal handling.

Animal husbandry and experimental procedures were performed in accordance with the guidelines of local authorities (Berlin, Germany), the German Animal Welfare Act and the European Council Directive 86/609/EEC. Animals were housed on a 12:12h day-night cycle with food and water available ad libitum. Constitutive CB_1R-, CB_2R-, and DAGLα KO mice (Buckley et al., 2000; Jenniches et al., 2015; Zimmer et al., 1999) were bred using a homozygous breeding protocol. Additionally, a subset of constitutive CB_2R KO mice was bred from heterozygous parents and their WT littermates were used as controls. Neuron-specific, conditional KO mice for CB_2R were generated using the Cre/loxP technology. To this purpose, transgenic mice expressing Cre recombinase under the Synapsin I promoter were bred with floxed CB_2R animals (see below). In this case, Cre-negative offspring was used as a control. DNA isolation and genotyping were performed according to standard protocols. All KO mice were maintained on a C57BL/6J genetic background.

Generation of conditional CNR2 knockout mice.

Two loxP sites were inserted into the Cnr2 gene flanking the coding exon 2 by homologous recombination into embryonic stem cells. An FRT-flanked neo selection cassette was also inserted upstream of the loxP site in the 3' untranslated region. Recombinant ES cell clones were identified by Southern blotting with flanking 5' and 3' probes. One clone was used for the generation of chimeric animals. Mice with the recombinant Cnr2-flox/neo locus derived from these chimeras were mated with a Flp-deleter strain in order to remove the PGK-neo selection cassette, resulting in a floxed Cnr2 locus (see Figure S3). To control for the specific expression of Cre under the Synapsin promoter, Syn-Cre mice were bred with the Rosa-26-Stop-tdTomato reporter line. Rosa-CAG-LSL-tdTomato-WPRE:deltaNeo has a loxP-flanked STOP cassette preventing transcription of the downstream red fluorescent protein variant (tdTomato). When bred to mice that express Cre recombinase, the resulting offspring will have the STOP cassette deleted in the cre-expressing tissue(s) resulting in expression of tdTomato (Madisen et al., 2010). The brains of the offspring were removed, snap-frozen in isopentane on dry ice and stored at -80°C until use. Brains were then embedded in Tissue-Tek® and consecutively sectioned at 16µm using a Leica cryostat and stored at -20°C until use. The sections were covered with Fluromont and images were acquired on a Zeiss Axioplan confocal microscope.

In vitro electrophysiology.

Slice preparation. Hippocampal slices were prepared from P21-P35 C57BL/6 and KO mice, and Wistar rats (where indicated). Animals were anesthetised with isoflurane and decapitated. Their brains were quickly removed and transferred to sucrose-based ice-cold artificial cerebrospinal fluid (aCSF) containing (in mM): 87 NaCl, 26 $NaHCO_3$, 50 Sucrose, 10 Glucose, 2.5 KCl, 1.25 NaH_2PO_4, 3 $MgCl_2$, 0.5 $CaCl_2$ for mice and 87 NaCl, 26 $NaHCO_3$, 75 Sucrose, 25 Glucose, 2.5 KCl, 1.25 NaH_2PO_4, 3 $MgCl_2$, 0.5 $CaCl_2$ for rats, respectively. Tissue blocks containing the hippocampus were mounted on a VT1200SVibratome (Leica, Germany) and horizontal slices of 300µm thickness were cut. Slices were subsequently stored for 1-5h in an interface chamber (Haas et al., 1979) at near-physiological temperature (~35°C) and superfused with aCSF containing (in mM): 119 NaCl, 26 $NaHCO_3$, 10 Glucose, 2.5 KCl, 1 NaH_2PO_4, 1.3 $MgCl_2$, 2.5 $CaCl_2$ (pH 7.4; 285-300mOsm; ~1ml/ min). All aCSF was equilibrated with 95% O_2 and 5% CO_2.

General setup. Individual hippocampal slices were transferred to a submerged chamber (Luigs and Neumann, Germany), perfused with aCSF (~5ml/ min, heated to 33-34°C) and visualised with infrared differential interference contrast optics on an Olympus BX-51 WI microscope. Extracellular field and patch-clamp recordings were performed with a MultiClamp 700A amplifier (Axon Instruments, USA) and monitored using an HM1507-3 oscilloscope (Hameg, Germany). Signals were filtered at 2-4 kHz, digitised at 5-10 kHz with 16-bit resolution using a BNC-2090 interface board (PCI 6035E A/D Board, National Instruments, USA) and recorded in IGOR Pro 5.0 (WaveMetrics Inc., USA) with custom-made plug-ins. Putative hippocampal principal cells were identified based on their location, morphology and electrophysiological properties. CA2 PCs were additionally filled with 30µM Alexa and post-hoc identified under a fluorescence microscope (Leica DMI4000 B, Germany) according to their dendritic arborisation. They can be distinguished from neighbouring CA3a PCs by their characteristic dendritic bifurcation close to the soma (Wittner and Miles, 2007).

Pharmacological agents. All drugs were purchased from Tocris (Germany) or Cayman Chemical (via Biomol, Germany). If not stated otherwise, experiments were performed in the continuous presence of $GABA_A$- and $GABA_BR$ blockers (1µM gabazine and CGP55845 respectively) to isolate excitatory transmission, and 100nM NBQX to prevent epileptiform activity. For recording $GABA_AR$-mediated eIPSCs, the aCSF was supplemented with 25µM D-AP5, 10µM NBQX and 1µM CGP55845 to block AMPAR-, NMDAR- and $GABA_BR$-mediated transmission respectively. Field recordings were performed in aCSF only. Additional drugs were bath applied to the whole slice. CBR (inverse) agonists used were the following: AM-251 (2-5µM), SR (1µM), 2-AG (10µM), WIN 55,212-2 (1µM) and HU-308 (1µM).

Whole-cell and perforated patch recordings. Patch pipettes were pulled from borosilicate filamented glass capillaries (Harvard Apparatus, UK; 1.5 mm OD) with a DMZ Universal Puller (Zeiss, Germany) and fire-polished to a final resistance of 2-3 MΩ for wc recordings. Pipettes were backfilled with filtered internal solution containing (in mM): 130 $KMeSO_3$ (or, in some experiments, 140 $KMeSO_4$), 10 KCl, 10 HEPES, 4 NaCl, 4 Mg-ATP, 0.5 Na-GTP, 5 phosphocreatine, 285–290 mOsm, pH was adjusted to 7.3 with KOH. For pp recordings, pipettes with a final resistance of 3-4 MΩ were tip-filled with the same internal solution. They were then backfilled with internal solution additionally supplemented with gramicidin (80µg/ml) which was prepared as a stock solution (20mg/ ml, diluted in DMSO) on the day of use. For experiments with intracellular application of the non-hydrolysable GDP analogue GDP-β-S, Na-GTP in the internal solution was replaced with GDP-β-S, which was added freshly on the day of use.

All recordings, unless indicated differently, were performed in current-clamp mode. The resting V_m and input resistance (R_{in}) were determined directly after establishing the wc configuration or, for pp recordings, when the access resistance (R_a) had stabilised. Experiments were only continued if cells had a resting V_m more hyperpolarised than -55mV (not corrected for liquid junction potential, LJP). The cells were further characterised by recording their membrane response / firing pattern to current injections of increasing strengths (-20 to +800pA, increment: 20-50pA, 1s). Afterwards, the V_m was adjusted to -60mV with continuous current injection if not stated otherwise. R_{in}, R_a and pipette capacitance were monitored continuously throughout the experiment and the latter two were compensated for using bridge balance and capacitance neutralisation. For pp recordings, only cells with a stable R_a below 60MΩ were used, with the exception of the dual pp experiments, where the control cell was used if a R_a below 100MΩ was achieved. Experiments were stopped if cells depolarised by more than 5mV or the R_a changed > 10% over the course of the recording.

Action potential protocols. The standard AP protocol used consisted of 15 trains with 50 APs each (750 APs, inter-stimulus interval: 10ms, inter-train interval: 20s). Individual APs were elicited by 2ms long, somatic current injections (1-2nA). The theta-burst protocol used to test the induction threshold of CA1 PCs consisted of 10 bursts of five stimuli (applied at 100Hz) with a 200ms inter-burst interval, repeated every 5s 60x (3000 APs). For the construction of the physiological spike train (PST), the unit activity of a putative CA3 place cell recorded in a rat

traversing a linear track rat was used (Diba and Buzsáki, 2008; Schmidt et al., 2009). More specifically, an AP protocol was implemented using a 5min stretch of inter-spike intervals of this cell's place field firing pattern. Because the PST stemmed from rat data, this dataset was acquired in rat accordingly.

Recordings of IPSCs. Pharmacologically isolated (25µM AP5 and 10µM NBQX), evoked IPSCs (denoted as eIPSCs in figures) were recorded in voltage-clamp configuration at a holding potential of -50 or -70mV (resulting in either out- or inward currents). The stimulation electrode (borosilicate glass, as above) was positioned in stratum radiatum of CA3 ~150µm away from the recorded cell (towards the hilar region of the dentate gyrus) and the experiment were only started when the evoked IPSCs displayed monosynaptic rise and decay kinetics. DSI was elicited by depolarising the cell to 0mV (3x 1s, 5s interval or 1x 5s). Cells that showed a >15% reduction in the amplitude of the evoked IPSCs after the depolarising step were considered DSI-positive. Pharmacologically isolated (25µM AP5 and 10µM NBQX), spontaneous IPSCs for the analysis of DSI were recorded with an internal solution containing 140mM KCl to reverse and increase the driving force for chloride and in the presence of 20µM carbachol to boost their frequency.

Recordings of synaptically evoked EPSPs and action potentials. To test for the change in spike probability of CA3 PCs before and after pharmacological CB_2R activation, a stimulation electrode was placed in stratum radiatum of CA3 and synaptic, glutamatergic responses (EPSPs) were evoked and recorded in current clamp in the continuous block of GABAergic transmission. The stimulation strength was adjusted to an initial spike probability of ~80%.

Extracellular field recordings. For field recordings, both the stimulation and recording pipette (borosilicate glass, as above; tip diameter: ~20µm) were filled with aCSF and placed in stratum radiatum of area CA3. Field EPSPs were evoked by stimulating presumptive associational/commissural fibres (duration: 100µs, frequency: 0.05Hz) using a stimulus isolator (Isoflex, A.M.P.I) and adjusted to 60% of the maximal amplitude. The fEPSP slopes were determined as dV/dt (in mV/ms) of 10 to 90% of the amplitude in each individual trace.

Data analysis. Data analysis was performed in IGOR Pro 6.12 using the IGOR analysis software package Neuromatic (www.neuromatic.thinkrandom.com). Statistical comparisons between groups were performed in GraphPad Prism (GraphPad Software, USA). Sample sizes are given as the number of experiments (n) and the number of animals (N). Individual membrane potential values (denoted as V_m in figures) were determined from a 10ms average around the detected minimum within a 100ms time window every 20s. The minimum average was taken to circumvent distortions due to the high spontaneous activity in CA3 PCs. V_m values are not corrected for LJP, which was calculated to be 10mV (JPCalcW, Molecular Devices; USA) (Barry, 1994) for the $KMeSO_3$-based internal solution. The R_{in} was calculated from a 50ms average of the steady-state V_m response to a hyperpolarising test pulse (400ms, -20 to -80pA). Given V_m values were normalised to a 1min baseline (3 values) before the AP induction protocol or, for drug application, to a 2min baseline. For summary time plots of the global V_m average, the individual values of all experiments were averaged per point in time; alternatively, the median (including 25^{th} and 75^{th} percentile) at a certain time point is calculated as the average of 1min (3 values/ experiment). For the analysis of spontaneous IPSCs (denoted as sIPSCs in figures), individual events were detected with a threshold-based algorithm in Neuromatic and a total of 5-10s were analysed for each time point. The amplitude of each event was defined as the 10ms average maximum within a 100ms time window after the stimulation. Examples show individual traces.

The distribution of data was assessed with the D'Agostino and Pearson omnibus normality test. Normally distributed data sets were compared with a two-tailed Student's t-test and values are expressed as mean±SEM. Nonparametric tests were used as indicated and data presented as median (including the 25^{th} and 75^{th} percentile). The averages of the change in membrane potential (ΔV_m) across cells were assessed with the appropriate paired tests (Student's t-test or, if indicated, Wilcoxon signed-rank test). Correlation analyses were carried out using either the Pearson (for data sampled from Gaussian distribution, indicated by r) or Spearman (nonparametric, indicated by r_s) correlation coefficient. Results were considered significant at $p<0.05$. The percentage of reactive cells in each experiment was calculated from a -2.1mV cut-off to facilitate the comparison between different (recording-)

conditions/manipulations. This cut-off was based on the mean of the wc hyperpolarisation (-1.8mV) plus its standard error (-0.3mV). To give a 'biologically relevant' estimate of the average ΔV_m, only the values of reactive cells are averaged for data sets in which washout in the wc configuration led to a skewed data distribution.

The electrophysiological analysis of the const. (1) and cre-dependent (2) CB_2R KO animals, were partially (1) and fully (2) performed in a blind and interleaved manner. In case of the const. CB_2R KOs, the results of cells from heterozygously bred WT and KO littermates, that were recorded and analysed blind, were not different from homozygously bred KO and C57BL/6 WT mice (Mann-Whitney test: P=0.8) and the data was thus pooled.

In vivo electrophysiology.

Wire array recordings. After one week of handling and habituation to the recording room, mice were implanted under isoflurane anesthesia with arrays of single tungsten wires (40µm, California Fine Wire Company) in the CA3 area (coordinates relative to bregma, anteroposterior: -1.94mm, lateral: 2.3mm, ventral: 2.15mm). Reference and ground electrodes were miniature stainless-steel screws in the skull above the cerebellum. Implanted electrodes were secured on the skull with dental acrylic. After one week of recovery, animals were placed in a 1x1m open arena and were allowed to explore freely during recordings. Electrodes were connected to operational amplifiers (Neuralynx, USA) to eliminate cable movement artefacts. Electrophysiological signals were differentially amplified, bandpass filtered (1-9000Hz) and acquired continuously at 30303Hz. After 1h of baseline recordings animals were injected with either vehicle (10mg/kg DMSO) or with HU-308 (10mg/kg, dissolved in DMSO) and were recorded in the arena for one more hour. After completion of the experiments, mice were deeply anesthetised and electrolytic lesions at selected recording sites were performed. Subsequently the animals were perfused intracardially with 4% PFA solution and decapitated. Brains were fixed, cut into 50µm slices and stained with cresyl violet for confirmation of recording sites.

Data analysis. Signal processing was carried out off-line by custom-written MATLAB algorithms. The LFP was processed by low-pass filtering and down-sampling of the wideband signal to 1250Hz. Phase-amplitude coupling of theta and gamma oscillations was assessed for epochs of theta oscillations with a theta/delta power ratio of at least five. The theta phase was obtained by Hilbert transformation of the 5-10Hz filtered signal. Gamma oscillation peaks were detected in the 30-85Hz and 65-120Hz band-pass filtered signal, and their amplitudes and theta phases were subsequently calculated. The gamma amplitude – theta phase modulation coefficient was computed as a correlation coefficient (Fisher z-transformed, Pearson's or Spearman's, depending on the distribution normality) between the gamma modulation depth (Wulff et al., 2009) and the theta/delta ratio-standardised amplitude of the concurrent theta oscillation. Power spectral density was computed using the multitaper method (NW 3, window size 1024) and standardised to the power in the 30-45Hz band during baseline recordings. The statistical significance of comparisons was determined by a two-way ANOVA (subject x treatment and subject x genotype).

In situ hybridisation and immunohistochemistry

Classical In situ hybridisation. Animals (WT, $CB_1R^{-/-}$, and $CB_2R^{-/-}$; 2 mice each strain) used in this experiment were matched for age (6-8weeks) and weight (20–30g). The const. $CB_2R^{-/-}$ mice are C terminal-deleted, in which the last 341bp on exon 3 are deleted that encode parts of the intracellular and extracellular third loops, transmembrane regions 6 and 7, and the intracellular C terminus (Buckley et al., 2000; Zhang et al., 2014). These animals were deeply anesthetised and transcardially perfused with saline, followed by 4% Paraformaldehyde (PFA). CB_2R-mRNA riboprobe was synthesised as described in our previous report (Zhang et al., 2014). The ISH procedures for hippocampal CB_2R mRNA expression were the same as reported previously (Lanciego et al., 2011; Zhang et al., 2014). To determine the phenotype of mCB_2R mRNA-expressing neurons in hippocampus, we used

fluorescent IHC to label all neurons with a NeuN antibody or glutamatergic neurons with a vGlut2 antibody, respectively. After the mCB_2R mRNA staining in freely floating coronal slices by classical ISH, the sections were incubated with a mouse anti-NeuN antibody (1:1,000; Millipore) or a mouse anti-vGlut2 antibody (1:500; Millipore) at 4°C overnight, followed by Alexa Fluor 488 goat anti-mouse IgG (1:500; Molecular Probes) at RT for 2h. The sections were mounted on glass slides, air-dried at RT, and coverslipped with Fluorogel and Tris buffer (Electron Microscopy Sciences).

RNAscope In situ hybridisation. Animals (WT, Syn- $CB_2R^{-/-}$, and $CB_2R^{-/-}$ mice; 2-3 mice each strain, age 4-8 weeks) were perfused with saline to wash out blood cells in the brains, and then quickly decapitated. The whole brains were taken out, quickly frozen on dry ice, and then stored at -80°C for CB_2R RNAscope ISH assays. The brains were sectioned coronally (14μm thick, -2.8mm posterior to bregma) to sample the hippocampus (Paxinos and Watson, 2005). The freshly frozen sections were then mounted on positively charged microscopic glass slides (Fisher Scientific). A CB_2R-specific probe (Mm-*Cnr2*-O2) that targets the *Cnr2* gene-deleted region on exon 3 (506-934bp of NM_009924.4) and a NeuN probe (Mm-*Rbfox3*-C2) that targets 1827-3068bp of NM_001039167.1 were designed and provided by Advanced Cell Diagnostics Inc. The CB_2R/NeuN mRNA staining was performed following the User Manual for Freshly Frozen Tissue using the RNAscope Multiplex Fluorescent Reagent Kit (Advanced Cell Diagnostics). Stained slides were coverslipped with fluorescent mounting medium (ProLong Gold Antifade Reagent P36930, Life Technologies) and scanned into digital images with an Olympus FluoView FV1000 confocal microscope at 60× magnification using manufacturer-provided software.

Fluorescence-activated cell sorting (FACS). The frozen, -80°C cold whole brains were then put into a -20°C cryostat to equilibrate for at least 30min before dissection. The dissection procedure was the same as reported previously (Li et al., 2015; Liu et al., 2014; Rubio et al., 2015) with very minor modifications. Briefly, 1.5mm thick coronal hippocampal sections were cut at the levels of bregma - 2.27 and - 3.77mm, and then hippocampal tissues were punched with a 24gauge neuron punch needle (Fine Science Tools). After finely mincing the hippocampal tissue with razor blades on ice, it was transferred into 1ml of ice-cold Hibernate A (HA-if, Brain Bits). After centrifuging at 3,000rpm (4°C) for about 2min, the supernatant was discarded and the pellets were re-suspended in 0.6ml of ice-cold Hibernate A. Each sample was first triturated 10x in series using fire-polished glass pipettes (with successively smaller diameters of 1.0mm and 0.4mm), and then the samples were triturated for additional two times with 0.4mm-diameter glass pipettes. Each trituration step consisted of triturating up and down at least 1x. After centrifuging for 5min at 3,500rpm (4°C), the collected cells were re-suspended with 0.5ml of ice-cold Hibernate A. The cell pellets were then fixed and permeabilised by adding the same volume of 100% of cold ethanol (-20°C) for 15min on ice. After centrifuging for 4min at 4,000rpm (4°C), the cell pellets were re-suspended with 0.5ml PBS and incubated with a PE-labeled (fluorescent) anti-NeuN antibody (1:500; FCMAB317PE, Millipore) at 4°C for 30min. Then the cells were washed 3x with 0.5-1.0ml cold PBS. After the cells were filtered with 40μm cell strainers (Falcon brand; BD Biosciences), NeuN-positive and NeuN-negative cells were sorted by a FACSAria I cell sorting system (BD Biosciences). The sorted neurons or cells can be identified by the distinct forward (FSC) and side (SSC) scatter properties. DAPI (1 μg/ml, staining DNA) staining indicated that 98% of the events in the neuronal gate are DAPI-positive events (nucleated cells). After defining the cell population, we gated single cells by FCS width and height, in which ~98% of single cells were DAPI positive. This single-cell population was sorted again to separate NeuN-positive hippocampal neurons (with PE fluorescent signal) and NeuN-negative non-neuronal cells (not PE fluorescent) (approximately 5000 cells for each group) for the following CB_2R mRNA qPCR assays. The sorted cells were collected into 1.5ml Eppendorf tube containing 50μl extraction buffers (PicoPure RNA isolation kit, Arcturus Bioscience) and then suspended by pipetting up and down 10x, followed by incubation at 42°C for 30min. After centrifuging the suspension at 3,500 at 4°C for 2min, the supernatant were collected for the RNA extraction according to the manufacturer's protocol for using PicoPure RNA isolation kit (Arcturus Bioscience) to extract RNA. After the RNA extraction, the cDNA was synthesised by use of Superscript III first strand cDNA synthesis kit (Invitrogen). We used gene-targeted preamplification of cDNA as described previously (Li et al., 2015; Liu et al., 2014; Rubio et al., 2015). First, we pooled TaqMan ABI primer/probes (20×TaqMan gene expression assay as a

stock solution) for all the target genes listed in Table 1. Each cDNA sample (10µl) was mixed with the pooled primer solution (10µl) and 20µl of 2×TaqMan PreAmp Master Mix (Applied Biosystems). The cDNA preamplification was performed in a Veriti 96-well Thermal Cycler (Applied Biosystem) using the following program: 95°C hold for 10min, denaturation at 95°C for 15s, and annealing and extension at 60°C for 4min (14 cycles). The preamplified cDNA product was diluted 10x before proceeding for qPCR assays. The qPCR was performed in duplicates with a FAM-labeled probe for each target gene and a VIC-labeled probe for an endogenous control gene (*Gapdh*). We used TaqMan Advanced Fast PCR Master Mix (7500 Fast TaqMan instrument, Life Technologies) for qPCR, using the following program: 95°C hold for 20s, then 40 cycles with denaturation at 95°C for 3s, and annealing and extension at 60°C for 30s. The ΔΔCt method with *Gapdh* as the housekeeping gene was used to analyse the PCR reactions. The uniformity of the preamplification was verified by comparing cDNA templates with the unamplified and preamplified samples (data not shown).

Table 1. **Related to experimental procedures.** Gene expression assays and primer or probe sequences for FACS

Gene **(Protein)**	**TaqMan probe[a] or Assay ID[b]/Cat. no[c]**	**Forward primer**	**Reverse primer**
Cnr2 (CB_2R)	ATGCTGGTTCCCTGCAC[a]	AGCTCGGATGCGGCTAGAC	AGGCTGTGGCCCATGAGA
Cnr1 (CB_1R)	Mm01212171_s1[b]		
Rbfox3 (NeuN)	Mm01248771_m1[b]		
Itgam (CD11b)	Mm00434455_m1[b]		
Cspg4 (NG-2)	Mm00507257_m1[b]		
Aldh1l1 (ALDH1L1)	Mm03048957_m1[b]		
Gapdh (GAPDH)	4352339E[c]		

Statistics analysis. Data is presented as mean ± S.E.M. One-way ANOVA was used to analyse the difference between WT and 2 CB_2R-KO mice in terms of different target gene expression in NeuN-positive and NeuN-negative cells. Individual group comparisons were carried out using the Student–Newman–Keuls method.

Supplemental references

Barry, P.H. (1994). JPCalc, a software package for calculating liquid junction potential corrections in patch-clamp, intracellular, epithelial and bilayer measurements and for correcting junction potential measurements. J. Neurosci. Methods *51*, 107–116.

Diba, K., and Buzsáki, G. (2008). Hippocampal network dynamics constrain the time lag between pyramidal cells across modified environments. J. Neurosci. *28*, 13448–13456.

Haas, H.L., Schaerer, B., and Vosmansky, M. (1979). A simple perfusion chamber for the study of nervous tissue slices in vitro. J. Neurosci. Methods *1*, 323–325.

Lanciego, J.L., Barroso-Chinea, P., Rico, A.J., Conte-Perales, L., Callén, L., Roda, E., Gómez-Bautista, V., López, I.P., Lluis, C., Labandeira-García, J.L., et al. (2011). Expression of the mRNA coding the cannabinoid receptor 2 in the pallidal complex of Macaca fascicularis. J. Psychopharmacol. *25*, 97–104.

Madisen, L., Zwingman, T.A., Sunkin, S.M., Oh, S.W., Zariwa, a H., Gu, H., Ng, L.L., Palmiter, R.D., Hawrylycz, M.J., Jones, A., et al. (2010). A robust and high-throughput Cre reporting and characterization system for the whole mouse brain. Nat. Neurosci. 13, 133–140.

Paxinos, G., and Watson, C. (2005). The rat brain in stereotaxic coordinates. (Elsevier Academic Press).

Rubio, F.J., Liu, Q.-R., Li, X., Cruz, F.C., Leao, R.M., Warren, B.L., Kambhampati, S., Babin, K.R., McPherson, K.B., Cimbro, R., et al. (2015). Context-Induced Reinstatement of Methamphetamine Seeking Is Associated with Unique Molecular Alterations in Fos-Expressing Dorsolateral Striatum Neurons. J. Neurosci. *35*, 5625–5639.

Schmidt, R., Diba, K., Leibold, C., Schmitz, D., Buzsáki, G., and Kempter, R. (2009). Single-trial phase precession in the hippocampus. J. Neurosci. *29*, 13232–13241.